Journal of Engineering Physics and Thermophysics, Vol. 72, No. 6, 1999

THEORETICAL STUDY OF THE CURVE OF THE MELTING POINT OF IRON WITH ALLOWANCE FOR IONIZATION BY PRESSURE

F. N. Borovik and G. S. Romanov

UDC 536.652, 539.89

A curve of the melting point of iron up to 200 GPa is constructed on the basis of the Lindemann criterion. The transverse velocity of sound, needed for determining the Debye temperature, is calculated with allowance for ionization by pressure. The compression dependence of the concentration of free electrons is ascertained via the band structure of the metal obtained for various compression ratios by solving the Hartree–Fock–Slater equations of a self-consistent field in the Wigner–Seitz approximation of spherical cells. The calculated curve is compared with the experimental melting-point curve.

Construction of wide-range equations of state of condensed media requires information on the behavior of thermodynamic characteristics at interfaces and the position of interfaces in the space of independent thermodynamic parameters. With iron taken as a case in point, we consider the behavior of one such interface, namely, the melting-point curve in the temperature-pressure plane.

Extensive experimental data on the melting of materials at increased pressures have now been amassed. Systematization of these data has led to the Simon equation [1, 2]

$$\frac{P - P_0}{a} = \left(\frac{T}{T_0}\right)^b - 1, \tag{1}$$

where P_0 and T_0 are the parameters of a distinguished point (most frequently the triple point), and the constants a and b are selected for best describing the experimental data in the assigned pressure range. This equation is a consequence of the assumption that the relation of the heat of fusion to the volume change in melting is adequately described by a linear pressure function. The latter does not hold, for example, for alkali metals, and for substances whose melting-point curve has an extremum, i.e., a point where the volume change in melting is equal to zero. For describing melting-point curves with extrema, study [3] suggested using a linear-fractional pressure function in lieu of a linear one, which leads to a generalization of the Simon equation and permits description of a wider class of materials.

Experimental data for high pressures (of the order of 100 GPa and higher) are much fewer in number. For iron, nickel, and copper there are data on the melting-point curve up to 500 GPa obtained on the basis of interpreting shock-wave measurements [4-6]. For iron, static measurements have been performed for pressures up to 200 GPa [7, 8]. It is found that the shock-wave measurements significantly overestimate melting points (by more than a thousand degrees). Among the causes of such overestimation, study [9] discussed, in particular, nonequilibrium effects.

Figure 1 plots an experimental curve of the melting point of iron (the solid line) based on data from [7, 8, 10]. Under normal conditions, iron melts at 1811 K. Here, it is in the δ-Fe phase and has a bcc structure. At 5.2 GPa and 1991 K, there is a triple point on the melting-point curve that corresponds to the triple quilibrium of δ-Fe–γ-Fe–liquid. The γ-Fe phase has an fcc structure. The slope of the curve of the melting point of δ-Fe is constant and equal to 0.035 K/MPa, i.e., the constant b in the Simon equation is equal to unity. The curve of the

Academic Scientific Complex "A. V. Luikov Heat and Mass Transfer Institute," National Academy of Sciences of Belarus, Minsk, Belarus. Translated from Inzhenerno-Fizicheskii Zhurnal, Vol. 72, No. 6, pp. 1162-1066, November–December, 1999. Original article submitted March 29, 1999.

1062-0125/99/7206-1025$22.00

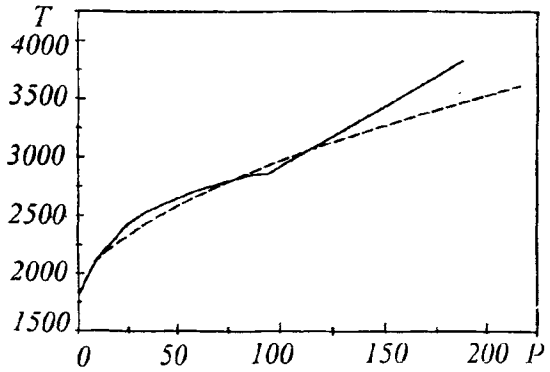

Fig. 1. Experimental (solid) and calculated (dashed) curves of the melting point of iron. T, K; P, GPa.

melting point of γ-Fe up to a pressure of 20 GPa is described by a parabola. At a pressure of 100 GPa there is a triple point [7, 8] that corresponds to the equilibrium of γ-Fe–α-Fe (or β-Fe)–liquid, and data are available on the presence, in its vicinity, of a new solid phase β-Fe instead of the α-Fe phase. At higher pressures, the melting-point curve is practically a straight line.

It is of interest to construct theoretically a melting-point curve for high energy concentrations. Study [11] qualitatively, with the aid of dimensional estimates, treated this problem on the basis of the Lindemann criterion, which asserts that the ratio of the mean amplitude of atomic (ion core) vibrations to the atomic spacing in a lattice at the melting point is a constant. In the Debye approximation, assuming the ion core vibrations near equilibrium positions to be classical, the Lindemann criterion is generally written as

$$\frac{MV^{2/3}\theta^2}{T_{\text{melt}}} = C^2. \tag{2}$$

Comparison with experimental melting points reveals that the constant C is equal to about 120–140 [1, 2], if the melting point and the Debye temperature are measured in degrees Kelvin. Study [2] proved that for systems whose potential energy is a uniform function of the coordinates the Lindemann relation ensues from self-similarity of the nonideal part of the statistical sum. Study [12] took into account the difference in the cold free energy for the solid and liquid phases in the melting region and so-called configuration entropy in the liquid. This permitted obtaining the Lindemann criterion under the assumption that the Grüneisen coefficient varies slightly along the melting-point curve. The relation of the Lindemann criterion to the vacancy mechanism of melting was considered in study [13], which obtained a relationship between the energy of vacancy formation in a close-packed metal and the Debye temperature and a formula according to which the melting point is proportional to the energy of vacancy formation. In turn, this energy is proportional to the energy of activation of self-diffusion in close-packed metals.

The Debye temperature is defined in terms of the mean velocity of sound for a specified lattice. At high energy concentrations, ionization by pressure occurs. Here, the charge of the ion cores and the concentration of the gas of free electrons vary, which causes a change in the vibration frequency of the ion cores. Study [14] showed that only the wave motions of ion cores with longitudinal polarization lead to fluctuations of the electron density, if no account is taken of so-called throw-over processes, where the electron quasimomentum after scattering by a phonon differs from the sum of the phonon momentum and the electron quasimomentum before scattering on the vector of the reciprocal lattice. These variations in the density of free electrons completely determine the longitudinal velocity of sound [15]. At temperatures where the electronic gas is degenerate it is possible to pass to the limit of zero temperature without loss of accuracy. For this case, study [15] obtained for the longitudinal velocity of sound c_{lon} the equation

$$c_{\text{lon}} = \left(\frac{Z_f m}{3M_{\text{at}}}\right)^{1/2} v_F. \tag{3}$$

Here, v_F is the velocity corresponding to the Fermi energy of the electronic gas, i.e., to the chemical potential at zero temperature. Application of Eq. (3) shows that using, for Z_f, the number of electrons with energy greater than zero leads to an overestimated velocity of sound. Much better results are obtained if the number of free electrons is calculated from the equation

$$Z_f = \frac{4}{3}\pi R^3 \rho_{el}(R). \tag{4}$$

Here, $\rho_{el}(R)$ is the total electron density at the cell boundary and R is the radius of a Wigner–Seitz spherical cell, specified by the material density. Such calculation of the number of free electrons was used in [16] for approximate account of the effect of strong repulsion of ions at high temperatures and densities on the thermodynamic parameters of the material. In the present study, $\rho_{el}(R)$ and v_F were ascertained with the aid of the Wigner–Seitz model of spherical cells, which was used for calculating zero isotherms up to superhigh compressions in [18]. In this model, the energy band structure of a crystal is computed on the basis of solving the Hartree–Fock–Slater equations of a self-consistent field under the assumption that the one-electron energy levels depend only on the magnitude of the quasimomentum and not on its direction. This approximation is justified for a compressed material, when close packing is realized. The Fermi velocity v_F is determined from the maximum kinetic energy of an electron at the cell boundary

$$E_k = E_F - U(R),$$

where E_F is the Fermi energy in a Wigner–Seitz cell and $U(R)$ is the potential energy at the cell boundary. It should be noted that $U(R) = 0$ if exchange interaction is disregarded.

For copper, under normal conditions Eqs. (3) and (4) yield the longitudinal velocity of sound $c_{lon} = 4837$ m/sec, whereas the experimental value is 4700 m/sec. For nickel, the agreement is somewhat worse, 5220 and 5630 m/sec. For iron, the theoretical value is 5737 m/sec, and the experimental, 5835–5960 m/sec. Hence the conclusion can be drawn that use of the model of spherical cells and Eqs. (3) and (4) at increased compressions is justified.

Calculation of the Debye temperature for a solid body also requires knowledge of the transverse velocity of sound, which differs markedly from the longitudinal (it is about half). As has been noted above, the interaction of ions and electrons affects the transverse velocity of sound slightly. Therefore, the effect of compression on the transverse velocity is elucidated using an approach from study [19], which treated the vibrations of a body-centered model lattice consisting of point ions and a negative charge spread uniformly over the crystal volume and due to electrons. The vibrations of ion cores were assumed not to deform the cloud of negative charge. Results presented in [19] permit determination of the transverse velocity of sound as a function of the number of free electrons and the compression ratio, i.e., the radius of a spherical cell:

$$c_t = D\frac{Z_f}{\sqrt{R}}. \tag{5}$$

The constant D in expression (5) can be ascertained from known Z_f, R, and c_t under normal conditions. As Z_f, we used previously calculated values. Now it is possible to find the mean velocity of sound c_m:

$$\frac{3}{c_m^2} = \frac{2}{c_t^2} + \frac{1}{c_{lon}^2}$$

and to introduce the Debye temperature for the lattice

$$\theta = \frac{h}{k}\frac{c_m}{\Omega^{1/3}}\left(\frac{3}{4\pi}\right)^{1/3}. \tag{6}$$

We next relate the Debye temperature to the melting point using the Lindemann criterion (2). This will make it possible, on specifying the specific volume and temperature and calculating the degree of ionization and the chemical potential of the electronic gas, to determine the mean velocity of sound and then find the Debye temperature from expression (6). Knowing these parameters and specifying the value of the constant C from Eq. (2) we obtain the melting point T_{melt}.

Calculations were carried out for iron, copper, and nickel. The constant C in Eq. (2) was evaluated from the condition that the calculated and actual melting points under normal conditions are equal. Since the Lindemann criterion does not involve the pressure, it is necessary to draw on a model equation of state of the material for comparison with experimental data. The current study uses the equation of state from [6], which accounts for both the cold pressure and heat pressure of ions and electrons. Figure 1 depicts the calculated curve of melting of iron (the dashed line). The initial section is not presented, since the curve is tied to the true melting point under normal conditions. The calculated curve was constructed using a single value of the constant entering the expression for the transverse velocity of sound, although the presence of triple points will undoubtedly lead to a change in it, since at a triple point the type of crystal lattice changes. The number of free electrons Z_f increases by about 25% as the pressure increases up to 200 GPa along the melting-point curve, being equal to 3 under normal conditions. It should be noted that for this pressure rise there is a corresponding compression of ≈ 1.7. The energy E_k changes 1.7-fold in this case.

On the whole, there is not only qualitative but also quantitative agreement between the calculated and experimental curves, despite the simplicity of the model employed.

Similar computations for nickel and copper showed that the calculated melting points are appreciably lower than the temperatures taken from [6]. Taking into account the good agreement between the experimental and calculated temperatures for iron, it is possible to conclude that the discrepancy for copper and nickel can be attributed to substantial arbitrariness in interpreting shock wave measurements.

The work was carried out under the program of the International Science and Technology Center, project B23-96.

NOTATION

P, pressure; P_0, pressure at the distinguished point; T, temperature; T_0, temperature of the distinguished point; a, b, constants in the Simon equation; M, atomic weight; V, molecular volume; T_{melt}, melting point; θ, Debye temperature; C, Lindemann constant; m, electron mass; M_{at}, atomic mass; Z_f, number of free electrons per atom; c_{lon}, longitudinal velocity of sound; c_m, mean velocity of sound; ρ_{el}, electron density; U, potential energy; E_k, kinetic energy of an electron whose total energy is equal to the Fermi energy; D, constant in Eq. (5); c_t, transverse velocity of sound; h, Planck constant; k, Boltzmann constant; Ω, volume per atom. Subscripts: m, mean; f, free; lon, longitudinal; t, transverse; k, kinetic; melt, melting.

REFERENCES

1. S. M. Stishov, *Usp. Fiz. Nauk*, **96**, Issue 3, 467-496 (1968).
2. S. M. Stishov, *Usp. Fiz. Nauk*, **114**, Issue 1, 3-40 (1974).
3. V. V. Kechin, *Zh. Fiz. Khim.*, **71**, No. 3, 391-394 (1997).
4. Q. R. Williams, R. Jeanloz, J. Bass, and T. J. Ahrens, *Science*, **236**, 181-182 (1987).
5. C. S. Yoo, N. C. Holmes, D. J. Webb, and C. Pike, *Phys. Rev. Lett.*, **70**, 3931-3934 (1993).
6. V. D. Urlin, *Zh. Eksp. Teor. Fiz.*, **49**, Issue 2 (8), 485-492 (1965).
7. S. K. Saxena, G. Shen, and P. Lazor, *Science*, **264**, 405-407 (1994).
8. R. Boehler, *Nature*, **363**, 534-536 (1993).
9. R. Boehler, *Phil. Trans. R. Soc. Lond.*, **A354**, 1265-1278 (1996).
10. E. Yu. Tonkov, *Phase Diagrams of Elements at High Pressure* [in Russian], Moscow (1979).
11. D. A. Kirzhnits, *Usp. Fiz. Nauk*, **104**, Issue 3, 489-508 (1974).

12. V. S. Vorob'ev, *Zh. Éksp. Teor. Fiz.*, **110**, Issue 2 (8), 683-695 (1996).
13. J. Enderby and M. March, in: *Phase Stability in Metals and Alloys* [Russian translation], Moscow (1970), pp. 28-46.
14. D. Pines, *Elementary Excitations in Solids* [Russian translation], Moscow (1965).
15. J. Bardeen and D. Pines, *Phys. Rev.*, **99**, No. 4, 1140-1150 (1955).
16. A. F. Nikiforov, V. G. Novikov, and V. B. Uvarov, *Teplofiz. Vys. Temp.*, **25**, No. 1, 12-21 (1987).
17. A. I. Voropinov, G. M. Gandel'man, and V. G. Podval'nyi, *Usp. Fiz. Nauk*, **100**, Issue 2, 193-224 (1970).
18. F. N. Borovik, A. M. El'yashevich, and G. S. Romanov, *Dokl. Akad. Nauk BSSR*, **31**, No. 2, 127-130 (1987).
19. C. B. Clark, *Phys. Rev.*, **109**, No. 4, 1133-1141 (1958).